JOURNAL

OF THE AMERICAN CHEMICAL SOCIETY

VOLUME 103, NUMBER 21 OCTOBER 21, 1981

Photoelectrochemical Oxidation of Sulfur Dioxide in Strong Acid Solution: Iodide-Mediated Oxidation at Illuminated Metal Dichalcogenide Electrodes

Gary S. Calabrese and Mark S. Wrighton*

Contribution from the Department of Chemistry, Massachusetts Institute of Technology, Cambridge, Massachusetts 02139. *Received March 2, 1981*

Abstract: In strong acid solution, n-type MoS_2, $MoSe_2$, or WS_2 can be used as a photoanode to effect the oxidation of SO_2 to SO_4^{2-}. The oxidation can be driven with visible light, $h\nu > 1.1$ eV, with an output photovoltage of ~0.6 V relative to $E_r(SO_4^{2-}/SO_2)$ in 6 M H_2SO_4. The oxidation of SO_2, however, requires the presence of I^- as a mediator serving to (1) alter the MY_2/liquid energetics to shift the band edges to a more negative potential to yield a photovoltage relative to $E_r(SO_4^{2-}/SO_2)$ and (2) improve the kinetics for SO_2 oxidation presumably through the intermediate formation of I_3^-. It is noteworthy that MY_2 is stable in the presence of strong acid, even concentrated H_2SO_4; the photooxidation of SO_2 can be sustained without photoanodic corrosion of the MY_2 at current densities of ~20 mA/cm^2 and at potentials ~0.6 V more negative than $E_r(SO_4^{2-}/SO_2)$. The cathode reaction is H_2 evolution, and the overall reaction is $2H_2O + SO_2 \rightarrow H_2SO_4 + H_2$ that comprises one part of a hybrid cycle for splitting H_2O to $H_2 + {}^1/_2O_2$. The cycle is completed, in principle, by thermolyzing H_2SO_4 to $H_2O + SO_2 + {}^1/_2O_2$. Thus, light and heat can be used to effect water splitting. Fundamentally, the noteworthy finding is that I^- allows a good rate (current) for SO_2 oxidation and also favorably affects the energetics to improve the photovoltage. This new concept may be exploited to illustrate processes that can be uniquely done at semiconductor photoelectrodes. The efficiency for conversion of 632.8-nm light (~50 mW/cm^2) in 6 M H_2SO_4/~1 M SO_2/5 mM I^- is ~8% using an n-type WS_2 photoanode.

Photoelectrolysis of SO_2/H_2SO_4 solutions according to reactions 1 and 2 is of possible importance in energy conversion, since the

$$SO_2 + 2H_2O \xrightarrow[\text{photoanode, } 2\ h\nu]{n\text{-type semiconductor}} H_2SO_4 + 2H^+ + 2e^- \text{ (anode)} \quad (1)$$

$$2H^+ + 2e^- \rightarrow H_2 \text{ (cathode)} \quad (2)$$

thermal decomposition of H_2SO_4 is known to proceed according to reaction 3 to give O_2.[1] The net reaction from reactions 1–3

$$H_2SO_4 \xrightarrow{\text{heat}} {}^1/_2O_2 + H_2O + SO_2 \quad (3)$$

is the decomposition of H_2O with optical and heat energy (reaction 4). The conventional electrochemical oxidation of SO_2 to SO_4^{2-}

$$H_2O \xrightarrow{\text{light, heat}} H_2 + {}^1/_2O_2 \quad (4)$$

is plagued by poor current density and large overvoltage.[2] In 50% by weight H_2SO_4 the electrolysis according to reactions 1 and 2 requires a minimum applied potential of ~0.3 V[2] which seems to be a good match to the photovoltage, E_V, that can be obtained from n-type semiconductor photoanodes having a band gap E_g, suitable for efficient solar energy conversion (E_g in the range 1.0–2.0 eV). We set out to attempt photoelectrochemical oxidation of SO_2 in acid solution at nonoxide, visible-light-responsive n-type semiconducting photoanode materials, in part because such electrodes have not yet proven to be capable of directly yielding O_2 from photooxidation of H_2O.

The difficulty in generating O_2 at nonoxide photoanodes has been that the electrodes suffer anodic decomposition when illuminated in aqueous electrolytes containing only H_2O as the electroactive solution species.[3] It is now well-known that redox reagents added to H_2O/electrolyte solutions can be oxidized completely competitively at nonoxide photoanodes, effectively suppressing the decomposition of the electrode.[3-6] Our initial hope was that SO_2 at high concentration would be oxidized in competition with photoanodic corrosion of the electrode. We purposefully chose n-type MoS_2 (E_g ~1.1 eV) as the photoanode, since its photoanodic decomposition is known to proceed according to reaction 5.[7] The hope was that the SO_2 would be preferentially

$$MoS_2 + 8H_2O \xrightarrow{\text{light}} Mo^{6+} + 2SO_4^{2-} + 16H^+ + 18e^- \quad (5)$$

oxidized to SO_4^{2-} in competition with the MoS_2. It is known that

(1) Farbman, G. H.; Parker, G. H. In "Hydrogen: Production and marketing"; Smith, W. N., Santangelo, J. G., Eds; American Chemical Society: Washington, DC, 1980; Adv. Chem. Ser. No. 161, p 359.
(2) Lu, P. W. T.; Ammon, R. L. *J. Electrochem. Soc.* **1980**, *127*, 2610.
(3) Wrighton, M. S. *Acc. Chem. Res.* **1979**, *12*, 303.
(4) Hodes, G.; Manassen, J.; Cahen, D. *Nature (London)* **1976**, *261*, 403.
(5) Miller, B.; Heller, A. *Nature (London)* **1976**, *262*, 680.
(6) Chang, K. C.; Heller, A.; Schwartz, B.; Menezes, S.; Miller, B. *Science (Washington, DC)* **1977**, *196*, 1097.
(7) Tributsch, H.; Bennett, J. C. *J. Electroanal. Chem.* **1977**, *81*, 97.

0002-7863/81/1503-6273$01.25/0

Scheme I. Interface Energetics for n-Type MoS_2 in Acid Solution without I^- (a) and with I^- (b)[a]

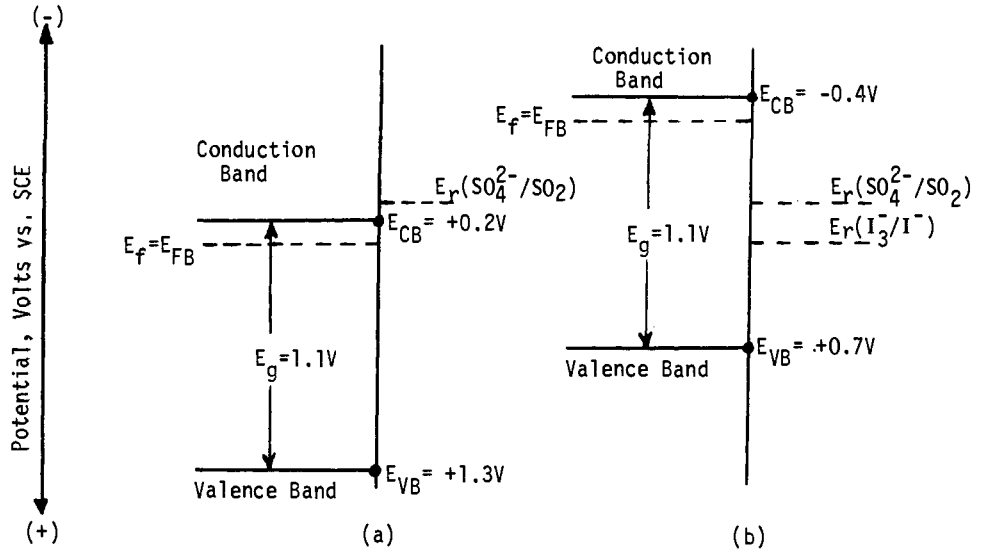

[a] E_{FB} is the so-called flat-band potential and E_{CB} and E_{VB} are the band edge positions. The $E_r(SO_4^{2-}/SO_2)$ is ~+0.2 V vs. SCE in 6 M H_2SO_4 while $E_r(I_3^-/I^-)$ is ~+0.3 V vs. SCE under the same conditions.

S^{2-} in solution will suppress photoanodic decomposition of CdS (E_g = 2.4 eV) (reaction 6) by being competitively oxidized to S_n^{2-}.[3]

$$CdS \xrightarrow{\text{light}} Cd^{2+} + S + 2e^- \quad (6)$$

Moreover, adsorption of S_n^{2-} onto CdS favorably affects the CdS/liquid interface energetics to give a large value of E_V.[8,9] A strong SO_2/MoS_2 interaction could favorably affect the expected E_V as well. Finally, the choice of MoS_2 is attractive, since it is a material that is known to be surprisingly durable in the presence of powerful oxidants despite its photoanodic decomposition in most aqueous electrolyte systems.[7,10]

A priori, a major drawback with the SO_2/MoS_2 system is that in the absence of SO_2 adsorption we would predict low optical to chemical energy conversion efficiency, η, since $E_r(SO_4^{2-}/SO_2)$ is close to a value where E_V is expected to be small or possibly zero. We take E_r to be the formal potential of the solution couple. The interface energetics for the MoS_2/liquid are expected to be as indicated in Scheme Ia in the absence of adsorption.[11] In the scheme E_{VB} and E_{CB} represent the positions of the top of the valence band and bottom of the conduction band, respectively, on an electrochemical scale, and E_f represents the electrochemical potential of the electrode. The value of E_f where the bands are flattened as shown is called the flat-band potential, E_{FB}. For solution redox couples having E_r more negative than E_{FB} the value of E_V is expected to be zero.[3,12,13] Thus, for the SO_4^{2-}/SO_2 system in 6 M H_2SO_4 $E_r \simeq +0.2$ V vs. SCE, and we cannot expect to be able to effect the uphill formation of SO_4^{2-} from SO_2 by illumination of the MoS_2. For an illustration of how adsorption may alter the situation, consider part b of Scheme I that illustrates the MoS_2/liquid interface energetics when I^- is present.[11,14] The effect of I^- adsorption is to shift E_{FB} more negative by ~0.6 V. For solution redox couples having E_r between E_{VB} and E_{CB}, E_V is expected to be nonzero and is given by eq 7 where E_{redox} is the

$$E_V = |E_{FB} - E_{redox}| \quad (7)$$

actual electrochemical potential of the solution. Thus, for the I_3^-/I^- redox couple a value of $E_V \simeq 0.5$ V can be obtained, whereas in the absence of I^- adsorption, as in nonaqueous CH_3CN/electrolyte solution,[11] E_V should be nearly zero.

Scheme II. Mechanism for I^- Mediated Oxidation of SO_2 in Acid Solution[a]

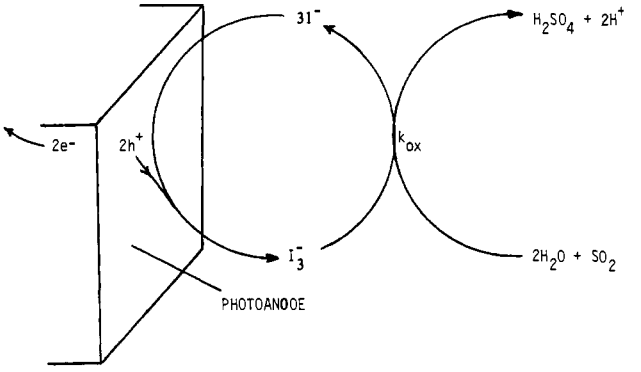

[a] Such a mechanism is classified as EC′ in the electrochemical nomenclature.[16]

With respect to the SO_4^{2-}/SO_2 couple, the consequences of adsorption by the I^- could be important. If SO_2 adsorption occurs E_{FB} could be favorably affected to give a good E_V. If SO_2 does not adsorb it may be possible to exploit the I_3^-/I^- system, since I_3^- is known to react with SO_2 according to reaction 8.[15] The

$$SO_2 + 2H_2O + I_3^- \xrightarrow{k_{ox}} H_2SO_4 + 2H^+ + 3I^- \quad (8)$$

I_3^-/I^- couple might then serve as a mediator system for the desired reaction as sketched in Scheme II. One question will be whether SO_2 is oxidizable by I_3^- with a large rate constant k_{ox} at acid strengths where $E_r(SO_4^{2-}/SO_2)$ is more positive than E_{FB}. The mediation system can only work if $E_{redox}(I_3^-/I^-)$ is more positive than $E_{redox}(SO_4^{2-}/SO_2)$ at the illuminated electrode. But the crucial question is whether SO_2 will interfere with the adsorption of I^- that provides for a nonzero E_V by shifting the value of E_{FB} to a more negative potential.

A comment on the determination of η is appropriate here. We take η, in %, to be given by eq 9, where E_V in volts is given by

$$\eta = (E_V i/I_n)100 \quad (9)$$

(8) Ellis, A. B.; Kaiser, S. W.; Bolts, J. M.; Wrighton, M. S. *J. Am. Chem. Soc.* **1977**, *99*, 2839.
(9) Ginley, D. S.; Butler, M. A. *J. Electrochem. Soc.* **1978**, *125*, 1968.
(10) Kubiak, C. P.; Schneemeyer, L. F.; Wrighton, M. S. *J. Am. Chem. Soc.* **1980**, *102*, 6898.
(11) Schneemeyer, L. F.; Wrighton, M. S. *J. Am. Chem. Soc.* **1979**, *101*, 6496; **1980**, *102*, 6964.
(12) Gerischer, H. *J. Electroanal. Chem.* **1975**, *58*, 263.
(13) Frank, S. N.; Bard, A. J. *J. Am. Chem. Soc.* **1975**, *97*, 7427.
(14) Tributsch, H. *J. Electrochem. Soc.* **1978**, *125*, 1086; Gobrecht, J.; Tributsch, H.; Gerischer, H. *ibid.*, **1978**, *125*, 2085.
(15) (a) Peters, D. G.; Hayes, J. M., Hieftje, G. M. "Chemical Separations and Measurements", Saunders: Philadelphia, PA, 1974, p. 328; (b) Killer, F. C. A.; Underhill, K. E. *Analyst* **1970**, *95*, 505.
(16) Bard, A. J.; Faulkner, L. R. "Electrochemical Methods"; Wiley: New York, 1980; pp 429-487.

eq 7, i is in amperes, and the optical power I_n is in watts. This expression is a representation of the efficiency for converting optical energy to chemical energy without regard to the process(es) occurring at the cathode. There are other ways to express efficiency, but this seems to be the best way to standarize measurements from laboratory to laboratory for given photoelectrode materials. Equation 9 is an expression of the efficiency for transducing optical power into electrical power to drive the oxidation of the solution species under consideration. In this case we are concerned with the SO_4^{2-}/SO_2 redox couple, not the mediator I_3^-/I^- couple. Thus, E_V is taken relative to $E_{redox}(SO_4^{2-}/SO_2)$ not relative to $E_{redox}(I_3^-/I^-)$. The extent to which $E_{redox}(SO_4^{2-}/SO_2)$ is more negative than $E_{redox}(I_3^-/I^-)$ represents a loss in E_V that must be sacrificed in order to have a large rate constant k_{ox}. The aim will be to have a sufficiently large k_{ox} that the quantum yield for electron flow, Φ_e, will be as high as possible without sacrificing any more E_V than is necessary.

Experimental Section

Materials. Samples of n-type MoS_2 and $MoSe_2$ were obtained and prepared for electrode fabrication as previously described.[11] Single crystals of n-WS_2 grown by vapor transport were kindly provided by Dr. Aaron Wold of Brown University and were prepared for fabrication in a similar manner.[17] Ohmic contact to the back side of the crystals was made by rubbing eutectic Ga-In and securing to a coiled Cu wire with conducting Ag epoxy. The Cu wire was passed through a 4-mm glass tube, and all surfaces were then sealed with Epoxi-Patch 1C white epoxy (Dexter Corp) so as to leave only the front surface (001) face of the crystals exposed. All chemicals were reagent grade. Anhydrous SO_2 was obtained from Matheson.

Equipment and Procedures. Current-voltage data were obtained by using either a PAR Model 173 or an ECO Model 551 potentiostat equipped with a PAR Model 175 programmer. Data were recorded on a Houston Instruments Model 2000 XY recorder or for current-time plots on a Hewlett Packard strip chart recorder.

Electrodes were illuminated with a beam-expanded Aerotech 632.8-nm polarized He-Ne laser. Laser intensity was varied by using a photographic polarizing filter and monitored with a beam splitter and a Tektronix J16 radiometer equipped with a J6502 probe. The laser beam was generally masked to match the size of the exposed crystal surface. Higher illuminations were obtained with a focused 200-W tungsten source.

Solutions were saturated with SO_2 by first purging with Ar or N_2, followed by bubbling with anhydrous SO_2 for at least 5 min. Approximate SO_2 concentrations were determined by titration with standardized triiodide solutions.[15] Two compartment electrochemical cells employed an ultrafine glass frit as separator. All counterelectrodes were Pt, and the reference electrode was a saturated calomel (SCE) electrode. Potentials vs. SCE in 6 M H_2SO_4 require a small correction (60 mV) for junction potential. The junction potential correction was determined by measuring the potential of a platinized Pt wire electrode in 6 M H_2SO_4 (1 atm H_2) vs. the SCE electrode. The measured value was -0.14 V vs. SCE. Using the activity of H^+ in 6 M H_2SO_4,[18] pH -2.8, and the Nernst equation we calculate $E_r(H^+/H_2)$ in 6 M H_2SO_4 to be $\sim$-0.08 V vs. SCE. Hence, all readings vs. SCE in 6 M H_2SO_4 should be corrected by 60 mV.

Results

Behavior of MY_2 Electrodes in 6 M H_2SO_4/SO_2 Solutions. The first noteworthy point is that single-crystal, n-type MoS_2, $MoSe_2$, and WS_2 are not thermally reactive in strong acid solution. Perhaps surprisingly we find no evidence whatsoever for liberation of H_2Y; the electrode materials are completely inert at 25 °C in the dark in 9 M H_2SO_4. Even when the solutions of acid are saturated with SO_2 ($\sim$1 M) we find no reaction of the MY_2 electrode materials. This gratifying result allows the investigation of the photoelectrochemistry of SO_2 under conditions where $E_r(SO_4^{2-}/SO_2)$ is more positive than E_{FB} when I^- adsorption occurs on MY_2. In 6 M H_2SO_4, the $E_r(SO_4^{2-}/SO_2) \sim +0.2$ V vs. SCE.

Study of the photoelectrochemical behavior of n-type MY_2 photoanodes in 6 M H_2SO_4 reveals that the MY_2 electrodes are photocorroded, as would be expected, when E_f is sufficiently positive.[7] Photocurrent corresponding to photoanodic corrosion onsets at $\sim$+0.4, $\sim$+0.3, and $\sim$+0.1 V vs. SCE for MoS_2, $MoSe_2$, and WS_2, respectively, in 6 M H_2SO_4 when the electrode is illuminated at 632.8 nm ($\sim$40 mW/cm^2). There is little or no current in the dark out to a positive potential of $\sim$+0.6 V vs. SCE in any case.

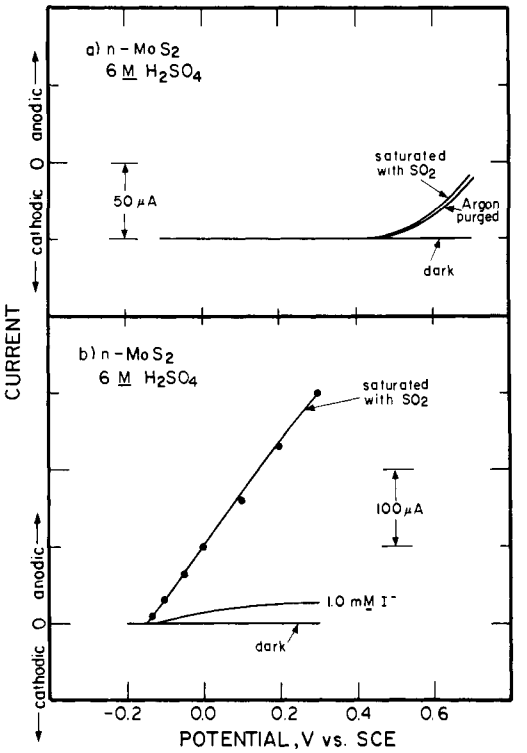

Figure 1. Representative steady-state current-voltage curves for a 0.07-cm^2 n-MoS_2 electrode illuminated with 632.8-nm ($\sim$40 mW/cm^2) light under the conditions shown. In (a) the curves were taken at 10 mV/s in stirred solutions and in (b) the points were obtained by holding at the indicated potentials for >60 s in a quiet solution while the smooth curve was taken at 10 mV/s in a stirred solution.

The saturation of 6 M H_2SO_4 with SO_2 results in a SO_2 concentration of $\sim$1 M. The photoanodic current from MY_2 electrodes is not significantly altered, either in magnitude or in onset, by the presence of the SO_2. Moreover, we do not find that SO_2 significantly affects the rate of photoanodic decomposition of MY_2. The SO_2 also does not result in any additional dark anodic current. Figure 1a shows typical current-voltage curve with and without $\sim$1 M SO_2 for illuminated MoS_2 in 6 M H_2SO_4. $MoSe_2$ and WS_2 behave similarly except that the onset of photocurrent is different.

I_3^-/I^- Mediated Oxidation of SO_2 at Illuminated MY_2 Electrodes. Figure 1b shows a typical photocurrent-voltage curve for MoS_2 in 6 M H_2SO_4 containing a low concentration of I^-. At the 1.0 mM I^- concentration and $\sim$40 mW/cm^2 the photocurrent is apparently limited by the mass transport rate of I^- and not by light intensity. The photocurrent observed depends on the stirring rate and is directly proportional to I^- concentration in the 0–5 mM I^- regime at a fixed stirring rate. Note that even at very low I^- concentration the photoanodic current onset is very negative compared to I^--free solution, consistent with the adsorption of I^- and the resulting negative E_{FB} previously reported at higher I^- concentrations.

Introducing $\sim$1 M SO_2 yields an onset of photocurrent that is about the same as for I^- alone, but the magnitude of the current is much greater and is independent of whether the solution is stirred. Thus, it would appear that the I_3^-/I^- couple can effectively mediate the oxidation of SO_2 to SO_4^{2-} as sketched in Scheme II. Qualitatively similar results are found for $MoSe_2$ and WS_2. Further, we find that the I_3^-/I^- system will mediate SO_2 oxidation at conventional Pt electrodes under the same conditions.

Figure 2 shows the photocurrent-voltage curves from illuminated MoS_2 for the $I^- \rightarrow I_3^-$ process alone and for the I_3^-/I^-

(17) The full characterization of n-WS_2, synthesis and photoelectrochemical behavior, is to be reported subsquently.

(18) Rochester, Colin H. "Acidity Funtions"; Academic Press: New York, 1970; Chapter 2.

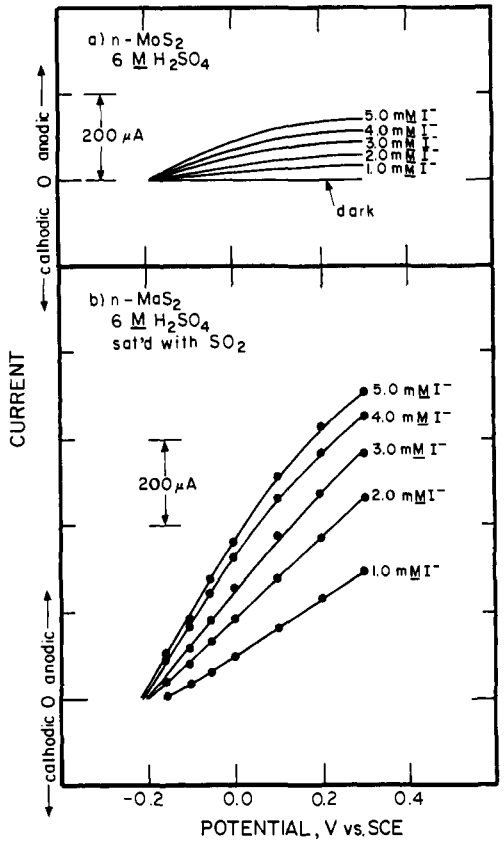

Figure 2. Representative steady-state current-voltage curves for a 0.07-cm² n-MoS_2 electrode illuminated with 632.8-nm (~40 mW/cm²) light under the conditions shown. The curves in (a) were taken at 10 mV/s in stirred solutions, and the points in (b) were obtained by holding at the indicated potentials for >60 s in quiet solutions.

mediated oxidation of ~1 M SO_2 as a function of I^- concentration at a fixed stirring rate. As indicated above, the photocurrent for I^- oxidation alone is directly proportional to I^- concentration at the light intensity used. At the lowest I^- concentration the photocurrent for the mediated oxidation of SO_2 is also proportional to the I^- concentration, but at higher I^- concentrations the photocurrent is limited, in part, by the light intensity in the ~40-mW/cm² regime. Qualitatively similar results are found for $MoSe_2$ and WS_2 photoanodes. At 2 mM I^- in 6 M H_2SO_4 and with ~50 mW/cm², the photocurrent for SO_2 oxidation was shown to be essentially independent of SO_2 concentration in the 0.25–1.0 M range.

The $E_r(SO_4^{2-}/SO_2)$ is dependent on acid concentration such that at greater acidity the E_r moves more positive. At very high acid strength the I_3^- may be thermodynamically incapable of oxidizing SO_2 to SO_4^{2-}. Figure 3 shows the photocurrent–voltage curves for illuminated MoS_2 in the presence of 1.0 mM I^- with and without ~1 M SO_2 and as a function of H_2SO_4 concentration. As the acid concentration is raised significantly beyond 8 M we find a sharp fall in the photocurrent associated with the mediated oxidation of SO_2. A similar fall in the mediated current is observed when using conventional Pt electrodes. The fall in mediated SO_2 oxidation current is attributable to insufficient oxidizing power of the I_3^-. The conclusion is confirmed by the observation at Pt that Br_2/Br^-, having an E_r of +0.8 V vs. SCE vs. $E_r(I_3^-/I^-)$ = +0.3 V vs. SCE, is capable of mediating the SO_2 oxidation even at 10 M H_2SO_4 whereas I_3^-/I^- is incapable of doing so. Table I summarizes the effect of varying H_2SO_4 concentration on the mediated oxidation of SO_2 by I_3^-/I^- from the three photoelectrodes used.

Durability of Photoanodes for Photooxidation of SO_2. The MY_2 photoanodes are remarkably durable under illumination in 6 M H_2SO_4 containing 5 mM I^- and ~1 M SO_2. SO_4^{2-} was determined to be the product of the photooxidation by carrying out the mediated SO_2 oxidation in 5 M HCl/5 mM I^-. The SO_4^{2-} produced from an illuminated MoS_2 electrode was determined gravimetrically by precipitation with Ba^{2+} to form $BaSO_4$. During the mediated oxidation the photocurrent density was ~20 mA/cm². The current efficiency for SO_4^{2-} production was determined to be >90% and >10 times as much SO_4^{2-} formed as could be accounted for by decomposition of the electrode according to reaction 5 with no detectable change in the electrode. In the same experiment >10 times as much SO_4^{2-} was formed as I^- initially present. No loss of I^- was detectable. In the absence of the I^- the photocorrosion of the electrodes is obvious after only several minutes of running at ~20 mA/cm² at a sufficiently positive value of E_f.

Table II summarizes several determinations of durability of the photoanode materials. In no case is phootoanodic corrosion detectable during mediated oxidation of SO_2. It is noteworthy that illumination of MY_2 results in the sustained, overall reaction represented by summing eq 1 and 2 (reaction 10), with no other

$$2H_2O + SO_2 \xrightarrow{\text{light}} H_2SO_4 + H_2 \qquad (10)$$

Table I. Effect of H_2SO_4 Concentration on Current for Mediated Oxidation of SO_2[a]

electrode	$[H_2SO_4]$, M	(current $I^- \rightarrow I_3^-$)/(current for $SO_2 \rightarrow SO_4^{2-}$)
MoS_2	5	8
	6	8
	7	4
	8	2
	9	1
$MoSe_2$	5	9
	6	8
	7	6
	8	2
	9	1
WS_2	5	8
	6	8
	7	5
	8	2
	9	1

[a] Data are culled from photocurrent-voltage curves like those shown in Figure 3. In all cases, the data are for 632.8 nm, ~40-mW/cm² illumination of the MY_2 photoanode in a cell having 1.0 mM I^- and ~1 M SO_2 with the indicated amount of H_2SO_4. The current ratio for $I^- \rightarrow I_3^-$ in the absence of SO_2 and for the mediated SO_2 oxidation is recorded at +0.3 V vs. SCE.

Table II. Summary of Durability Data for n-MY_2 Photoanodes for SO_2 Oxidation

sample[a]	initial crystal weight, g	charge passed, C	turnover no.[b]	current density, mA/cm²	condition[c]
n-MoS_2	0.038	10	1.5	4	+0.2V vs. SCE
n-MoS_2	0.018	500	22	20	+0.3V vs. SCE
n-WS_2	0.002	70	44	10	0.0V vs. SCE
n-WS_2	0.002	40	25	5	−0.2V vs. SCE[d]
n-WS_2	0.005	350	91	30	unbiased[e]
n-WS_2	0.004	260	83	40	unbiased[f]

[a] All runs were made in two-compartment cells with an ultrafine glass frit separator. Unless noted otherwise, the anode compartment contained 5 mM I^-/6 H_2SO_4 saturated with SO_2. The cathode compartment consisted of a Pt wire immersed in 6 M H_2SO_4. [b] Turnover no. = moles of SO_4^{2-} produced/moles of crystal initially present. No determination of MY_2 was found; thus the turnover numbers are minimum values. [c] Illumination was provided by a beam expanded He-Ne laser providing ~40 mW/cm². For higher current densities (~10 mA/cm²) illumination was from a focused 200-W tungsten source. The electrode was potentiostatted to the indicated potential except for the last two entries. [d] This run involved the use of 2 mM I^- in the anode compartment. [e] The photoanode was short circuited through a 49-Ω precision resistor to a Pt counterelectrode from which 42 mL of H_2 was collected (>95% current efficiency).

Table III. Representative Efficiencies for the Photoelectrochemical Oxidation of SO_2[a]

sample (no.)	input power, mW[b]	Φ_e at E_{redox}[c]	E_V max, mV	E_V at η_{max}, mV	η_{max}, %	fill factor
n-MoS_2 (1)	0.05	0.69	460	260	5.2	0.32
	0.10	0.64	480	260	5.2	0.33
	0.30	0.44	500	260	3.4	0.30
	0.50	0.33	510	260	2.4	0.28
	1.00	0.19	520	260	1.4	0.28
	1.50	0.13	530	260	1.0	0.28
n-MoS_2 (2)	0.05	0.74	420	240	7.2	0.45
	0.10	0.73	460	240	6.6	0.39
	0.30	0.65	490	240	5.0	0.30
	0.50	0.49	500	240	3.7	0.30
	1.00	0.30	520	240	2.3	0.29
	1.50	0.22	520	240	1.6	0.29
n-MoS_2 (3)	0.05	0.59	430	200	3.6	0.28
	0.10	0.59	460	200	3.6	0.27
	0.30	0.42	490	200	2.7	0.26
	0.50	0.33	500	200	2.1	0.25
	1.00	0.21	510	200	1.4	0.25
	1.50	0.16	520	200	1.1	0.25
n-$MoSe_2$ (1)	0.05	0.88	430	250	7.0	0.36
	0.10	0.86	460	250	7.1	0.36
	0.30	0.73	490	250	6.1	0.33
	0.50	0.65	510	250	5.3	0.31
	1.00	0.54	530	250	3.5	0.24
	1.50	0.46	540	250	2.9	0.23
n-$MoSe_2$ (2)	0.05	0.90	430	200	7.0	0.35
	0.10	0.90	450	200	6.5	0.31
	0.30	0.77	480	200	5.0	0.26
	0.50	0.65	500	200	4.0	0.24
	1.00	0.43	510	200	2.5	0.22
	1.50	0.31	520	200	1.8	0.22
n-WS_2 (1)	0.05	0.74	550	400	12.0	0.55
	0.10	0.73	560	400	12.0	0.56
	0.30	0.63	580	400	9.4	0.51
	0.50	0.60	590	400	8.6	0.47
	1.00	0.55	600	360	6.3	0.37
	1.50	0.50	600	350	5.0	0.32
n-WS_2 (2)	0.05	0.88	540	400	13.2	0.54
	0.10	0.88	560	400	12.0	0.48
	0.30	0.81	580	400	9.7	0.40
	0.50	0.76	590	400	7.6	0.33
	1.00	0.66	600	400	5.2	0.26
	1.50	0.53	600	400	4.0	0.25

[a] In all cases the solution contains 6 M H_2SO_4/~1 M SO_2 and 5 mM I^-. Input optical power is from a 632.8-nm source. [b] For power density multiply indicated values by 125 cm^{-2}. [c] $E_{redox}(SO_2/SO_4^{2-}) = +0.2$ V vs. SCE. Quantum yields are not corrected for reflection losses. Error limits are ±15%. [d] Fill factor is $[(\Phi_e @ \eta_{max})(E_V @ \eta_{max})]/[(\Phi_e @ E_{redox})(E_V \text{ max})]$.

energy input other than light. The data show nearly 100 mol of H_2 produced per mole of MY_2 without any detectable loss of electrode or deterioration in output parameters (±5%). Thus, we conclude indefinitely long lifetimes of the photoanodes at quite high photocurrent densities. For the reasons indicated above, the output parameters are expected to deteriorate significantly if the H_2SO_4 concentration exceeds 8 M (Figure 3 and Table I).

Efficiency for Photoelectrochemical Oxidation of SO_2. Using the definition of efficiency given in the introduction (eq 9), we find very good energy conversion efficiency for the mediated oxidation of SO_2 in acid solution (Table III). Data are included for various samples of the MY_2 electrodes and for different 632.8-nm light intensities. By virtue of the larger values of E_V and the better fill factors, the WS_2 samples give the highest efficiency. Higher light intensities generally give lower efficiency. The larger E_V's are more than offset by a diminution in Φ_e and fill factor at the higher light intensity. The visible light intensity from the AM 1 solar spectrum is ~50 mW/cm^2, and thus the efficiency entries in the 0.3 (~40 mW/cm^2) and 0.5 mW (~65 mW/cm^2) are a guide to what can be expected in terms of E_V and fill factor under AM 1 solar illumination. Efficiencies for conversion of solar energy at AM 1 will be at least a factor of 2 lower than those given in Table III for monochromatic 632.8-nm light.

Photoelectrochemical Processes Mediated by I_3^-/I^- at Illuminated MY_2 Electrodes. Since I_3^- is capable of being generated at MY_2 photoanodes it would seem rather straightforward to extend our results for the SO_2 system to other molecules that can be oxidized by I_3^-. However, the I_3^-/I^- couple at the MY_2 electrodes is a very special situation in that it is the strong interaction of I^- (and possibly I_3^-) with the MY_2 electrodes that allows the photogeneration of I_3^- to be an efficient process in terms of converting light to electricity (Scheme I). The point is that in order to effect the mediated photoelectrochemical oxidation of a reagent, A, using the I_3^-/I^- system, the reagent A or its oxidation product(s) must not interfere with the adsorption of the I_3^-/I^- system. One set of experiments illustrates that we are not raising a trivial issue.

Attempts to mediate the oxidation of thiosulfate, $S_2O_3^{2-}$, at illuminated MY_2 electrodes illustrates the problem. It is well-known that iodine should be capable of rapidly oxidizing $S_2O_3^{2-}$,[19] and we therefore attempted the mediated oxidation of $S_2O_3^{2-}$ in the same way that we had done the SO_2. The experiments were carried out in neutral, aqueous solutions, since the $S_2O_3^{2-}$ is not stable in strong acid. Figure 4 illustrates for n-WS_2 photoanodes what results when attempting to effect the I_3^-/I^- mediated photoelectrochemical oxidation of $S_2O_3^{2-}$. What is found is that the

(19) The formal potential for the $S_4O_6^{2-}/S_2O_3^{2-}$ couple is −0.16 V vs. SCE.[15a] The I_3^-/I^- couple should then be thermodynamically capable of mediating the oxidation of $S_2O_3^{2-}$. The $S_2O_3^{2-}$ is unstable in acid media and iodine titrations are best carried out in neutral media.

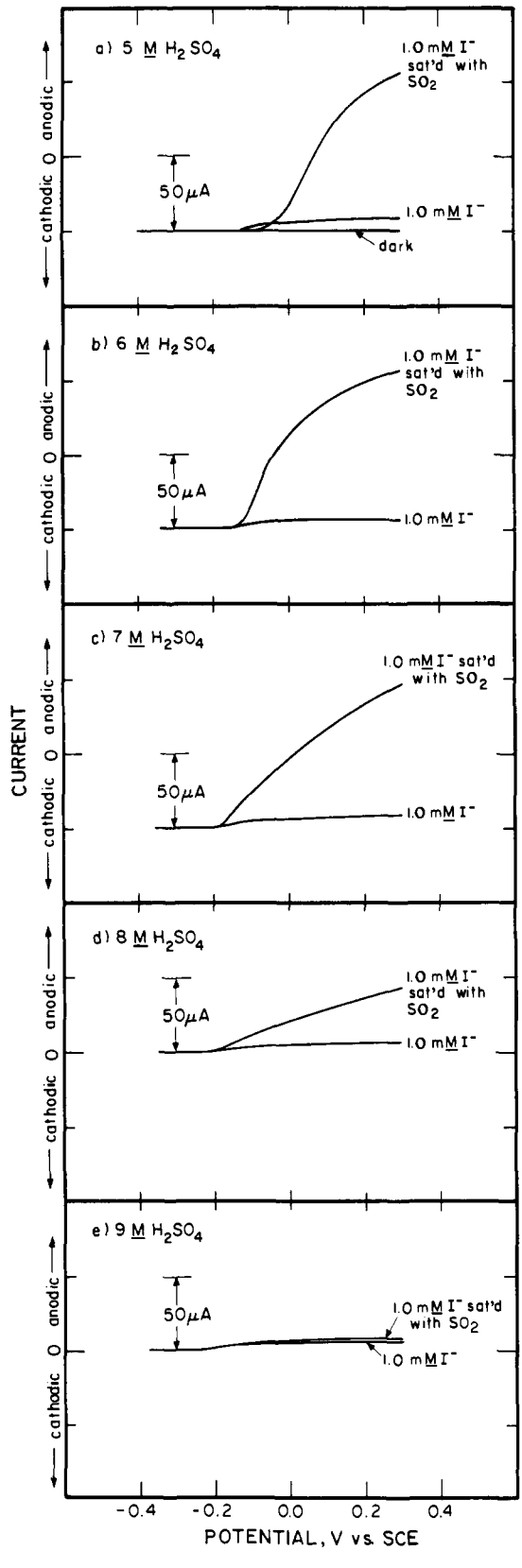

Figure 3. Steady-state current–voltage curves for a 0.07-cm^2 n-MoS_2 electrode illuminated with 632.8-nm (~40 mW/cm^2) light under the conditions indicated. Data show that at high H_2SO_4 concentration that the I_3^-/I^- does not effectively mediate the oxidation of SO_2 to SO_4^{2-}. In all cases the solutions are stirred.

behavior of the I^- alone in 0.1 M KCl is very similar to that of I^- alone in 6 M H_2SO_4. However, upon adding 1.0 M $S_2O_3^{2-}$ to the 5 mM I^-/0.1 M KCl solution, the onset of photoanodic current

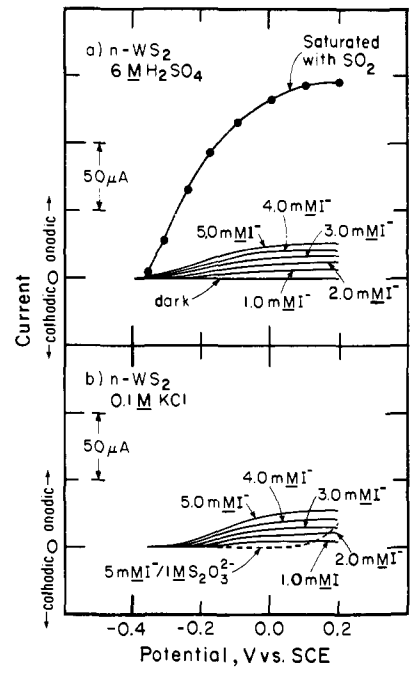

Figure 4. (a) Mediated SO_2 oxidation at illuminated (632.8 nm, ~40 mW/cm^2) n-WS_2 electrode. The SO_2 mediation is with 5 mM I^-. The I^- is oxidizable alone with a photocurrent that is proportional to I^- concentration in the 0–5 mM regime. (b) Attempted mediated oxidation of 1 M $S_2O_3^{2-}$. The 1 M $S_2O_3^{2-}$ suppresses the oxidation of I^-, and little or no mediated oxidation of $S_2O_3^{2-}$ occurs.

shifts more positive, and we do not see significant current for the mediated oxidation of $S_2O_3^{2-}$. This is in striking contrast to the experiment where ~1 M SO_2 is added to the 5 mM I^-/6 M H_2SO_4 solution where the onset is the same but much additional current is observed. Similar results obtain for MoS_2 and $MoSe_2$ for the $I_3^-/I^-/S_2O_3^{2-}$ system.

The point to make from the experiments summarized in Figure 4 is that for A = $S_2O_3^{2-}$ the favorable effect from the $MY_2/I_3^-/I^-$ interaction is destroyed by the $S_2O_3^{2-}$. However, for A = SO_2 there is apparently little or no effect on the interface energetics from the presence of ~1 M SO_2. It would appear that $S_2O_3^{2-}$ or decomposition products competitively bind to the MY_2 electrodes or at least prevents I^- or I_3^- from doing so. General use of the I_3^-/I^- mediator system at MY_2 will then depend on the preservation of the favorable effect on the interface energetics from the $MY_2/I_3^-/I^-$ interaction.

Discussion

We have adequately demonstrated that visible light can be used to drive the overall process represented by reaction 10 according to the mechanism represented by Scheme II where the photoanode materials are MoS_2, $MoSe_2$, and WS_2. The I_3^-/I^- mediation system is not sufficiently powerful thermodynamically that driving the formation of H_2SO_4 to a concentration of greater than 8 M is practically viable. The I_3^-/I^- mediation system for SO_2 oxidation works as well for conventional electrode materials and allows the demonstration of higher current densities for SO_4^{2-} formation at lower voltages than have previously been reported.

Perhaps surprisingly we do not find that the chemistry represented by reaction 11[20] alters the I_3^-/I^- mediator system. That

$$SO_2 + I^- \rightleftarrows SO_2I^- \quad (11)$$

is, we do not see the onset for the mediated SO_2 oxidation at a potential that is significantly different from that for the I^- oxidation alone. It is possible that SO_2I^- is in fact the electroactive species, but we have no direct evidence for this.

(20) Eller, P. G.; Kubas, G. J. *Inorg. Chem.* **1978**, *17*, 894.

The detailed mechanism for SO_4^{2-} formation likely involves the intermediate formation of SO_2I_2 or a related species that is then hydrolyzed.[21] Such a species would likely be much more hydrolytically labile than the SO_2Cl_2 that is known to hydrolyze to form SO_4^{2-}. In concentrated H_2SO_4 where the H_2O content is diminished it is possible that the rate of hydrolysis of the SO_2X_2 could be the rate-limiting step in the formation of SO_4^{2-} by X_2/X^- mediation. But for X = I the maximum concentration of H_2SO_4 that could be generated is too low to make hydrolysis of a species such as SO_2I_2 the rate-limiting step in forming SO_4^{2-} at 25 °C.

A major finding in this work is the demonstration that a mediator system can be found that not only allows the overall rate of redox reaction to be improved but also allows the reaction to be driven uphill under illumination. In the present instance, the oxidation of SO_2 at the MY_2 electrodes should occur in the dark, since $E_r(SO_4^{2-}/SO_2)$ is near the value of E_{FB} of the electrodes. In fact, no oxidation does occur in the dark, presumably because the kinetics are poor. The I_3^-/I^- mediator system not only improves the kinetics but the adsorption of the mediator also changes the interface energetics to give a good value of E_V for the SO_4^{2-}/SO_2 couple. The extent to which the adsorption/mediation by I_3^-/I^- can be exploited will depend on the extent to which the oxidizable substrate interferes with the adsorption. The attempts to photoelectrochemically mediate $S_2O_3^{2-}$ oxidation by the I_3^-/I^- system clearly illustrate the difficulties that can arise with such interferences. The findings with the $I_3^-/I^-/SO_2$ system suggest that it may be possible that there are combinations of reagents that will make the semiconductor photoelectrochemical approach the method of choice. Specific reagent/semiconductor interactions may make semiconductor electrodes the only electrodes that will enable certain redox reactions to be effected.

In the present instance of I_3^-/I^- mediated SO_2 oxidation the semiconductor photoelectrodes are not necessarily the electrodes of choice, since conventional electrodes can be used for the $3I^- \rightarrow I_3^-$ conversion. In such a case, the direct photoelectrochemical approach would have to compete with an approach where electricity, perhaps from photovoltaics, would be used to drive the reaction represented by reaction 10. It is widely belived that useful solar devices must achieve efficiencies in the vicinity of 10% in order to be practical.[22] The efficiencies in Table III suggest that the direct photoelectrochemical approach to effecting reaction 10 is about a factor of 2 away from the break-even point. Further, the photoanode materials are single crystal and relatively small in total exposed area. The promising result is that reaction 10 can be driven to a significant extent with durable, visible-light-responsive electrodes.

The variation in efficiency among MoS_2, $MoSe_2$, and WS_2 and various samples is significant. It is well-known that the efficiency from the MY_2 electrodes is a strong function of the surface properties.[11] The main finding is that n-WS_2, giving the highest values of E_V, gives the greatest efficiency. But even with this material there is room for improvement in some of the fundamental parameters such as fill factor. An important loss in every case is the reflection loss from the specular reflection of the single-crystal electrode materials. Much of the loss in Φ_e at E_{redox} is due to reflection loss. For WS_2, the improvement that could be gained from overcoming this loss would push the efficiency close to the 10% value.

Since we have shown that it is possible to effect H_2 generation at the cathode of our two compartment cell, it would be argued that higher efficiency could be obtained by just photoelectrolyzing HI (reaction 12). In fact, the basic efficiency should be improved

$$2HI(aq) \rightarrow H_2(g) + I_2(aq) \qquad (12)$$

to the extent that we do lose E_V equal to the difference in the $E_{redox}(I_3^-/I^-)$ and $E_{redox}(SO_4^{2-}/SO_2)$. However, in the formation of SO_4^{2-} we do not build up a colored product that will absorb the incident light. Nor is the reversion of SO_4^{2-} to SO_2 viable. Further, it is not clear that the abundance of iodine is sufficiently great that large-scale energy systems could be developed using it. Finally, the synthesis of H_2SO_4 provides an in principle path to the solar-induced splitting of H_2O, and H_2O clearly is sufficiently abundant for large-scale fuel generation.

Scheme III. Full Cell for Photoelectrochemically Driven Formation of H_2 and H_2SO_4 from SO_2 and $2H_2O$ in 6 M H_2SO_4 Using a WS_2 Photoanode and a Pt Cathode with I^- in the Anode Compartment as a Mediator[a]

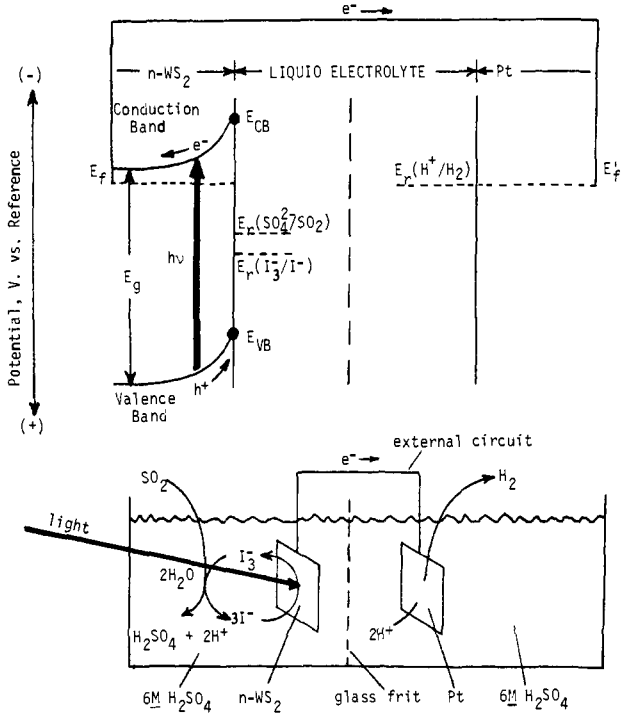

[a] At short circuit under illumination the electrochemical potential of both electrodes is at $E_r(H^+/H_2)$. For WS_2 photoanodes this value of E_f corresponds closely to the point where optimum efficiency can be obtained. Sufficient band bending obtains to have a high quantum yield (Figure 4a and Table III).

The ability to photoelectrochemically produce H_2 at the cathode of our two compartment cells, and without additional electrical energy particularly in the case of WS_2, is possible since $E_r(H^+/H_2)$ in 6 M H_2SO_4 is −0.1 V vs. SCE. As shown in the figures and Table III the onset of anodic current at the photoelectrodes is more negative than $E_r(H^+/H_2)$. Consequently, the electrons excited to the conduction band are capable of reducing H^+ to form H_2 at the counterelectrode. Scheme III illustrates the full cell energetics for the two compartment cell in 6 M H_2SO_4. The separator is necessary, since SO_2 reduction is a possible interference at the reducing potentials available. However, the separator does not have to be sophisticated or perfect and does not seem to be a difficulty. In our experiments we have synthesized ~50 mL of H_2 from a cathode compartment separated from the anode by a glass frit. Small concentrations of I^- in the cathode compartment do not seriously affect the H_2 evolution properties, and apparently there is little interference from SO_2 that might be present. The current efficiency for H_2 is determined to be ~100%.

The differences among MoS_2, $MoSe_2$, and WS_2 are likely due in large part to the fact that E_{FB} is somewhat different for each material. The E_{FB} for WS_2 is most negative followed by $MoSe_2$ and then MoS_2, as determined by the onset for current for the oxidation of I^- in 6 M H_2SO_4. The more negative E_{FB} results in the larger E_V for SO_2 oxidation; the excited electrons have greater reducing power. For WS_2 the E_f ~ −0.1 V vs. SCE (Scheme III) is very close to the E_f where the maximum value of η occurs. For MoS_2 and $MoSe_2$, E_f ~ −0.1 V vs. SCE is somewhat negative of the so-called maximum power point. Thus, these two electrodes are not nearly as efficient as WS_2 for reaction 10 when light is

(21) Witekowa, S.; Lewicki, A. *Rocz. Chem.* **1963**, *37*, 91. Note also that SO_2I_2 can be formed at −15 °C in SO_2 by addition of I_2: Jander, J.; Tuerk, G. *Angew. Chem.* **1963**, *75*, 792.

(22) Ehrenreich, H. "Solar Photovoltaic Energy Conversion"; The American Physical Society: New York, 1979.

the only energy input, since each of the electrodes in such a cell will be at the reversible H^+/H_2 potential (Scheme III) when the electrodes are short circuited under illumination.

Considering all of the direct photochemical fuel-producing systems,[23] the WS_2-based cell for driving reaction 10 stands quite high: (1) the system is durable; (2) visible light efficiency is respectable; (3) starting reagents are abundant and inexpensive; (4) the rate of conversion can be quite high; (5) the products that are generated are useful. It is particularly noteworthy that the WS_2 photoanode operates at nearly optimum efficiency when short circuited to a reversible H_2 electrode. That is, the value of E_V at the so-called maximum power point of the photocurrent-voltage curve is nearly equal to $E_r(H^+/H_2)$, providing a near perfect match to the potential needed to effect the overall process represented by reaction 10 when the cathode has little overvoltage as is the case with Pt.

(23) (a) Wrighton, M. S. *Chem. Eng. News* **1979**, *57*, No. 36, 29. (b) Bolton, J. R. *Science* (Washington, D.C.) **1978**, *202*, 705.

Acknowledgment. We thank the United States Department of Energy, Basic Energy Sciences, Chemical Sciences Division, and the Dow Chemical Company for support of this research.

^1H and ^{13}C ENDOR Investigations of Sterically Hindered Galvinoxyl Radicals†

B. Kirste, W. Harrer, H. Kurreck,* K. Schubert, H. Bauer, and W. Gierke

Contribution from the Institut für Organische Chemie der Freien Universität Berlin, 1000 Berlin 33, West Germany. *Received February 20, 1981*

Abstract: A variety of overcrowded novel galvinoxyl radicals have been synthesized. Steric requirements of bulky substituents have been studied by means of ESR, ENDOR, TRIPLE, and ENDOR-induced ESR spectroscopy. From ^1H and ^{13}C ENDOR measurements in nematic and smectic phases of liquid crystals anisotropic hyperfine contributions could be determined. The results suggest that steric interactions cause different geometrical arrangements within the galvinoxyl moiety. It is shown that one of the galvinoxyls exists in two stable conformations which can be discriminated by ENDOR-induced ESR. In case of significantly *differently* twisted aroxy rings (0-30°/80°) the galvinoxyl radical resembles a phenoxyl-type radical with equilibrating quinoid/benzoid rings rather than being a real delocalized system. This is accompanied by unusual relaxation properties of the central carbon atom.

ENDOR and TRIPLE resonance techniques have proved to be not only useful for the investigation of the static properties of organic radicals but also can be extended to the studies of temperature-dependent geometrical changes, e.g., in hybridization, or rapid structural interconversions.

Since dynamic intramolecular processes can affect widths and positions of spectral lines, detailed knowledge of the mechanisms involved in these dynamics is an essential prerequisite for an unambiguous analysis of complex ESR and ENDOR spectra. In recent papers we have shown that the spectra of galvinoxyl radicals are significantly altered when bulky substituents are introduced.[1-3] We have now prepared several novel galvinoxyls with different space-filling substituents. This enabled us to study steric effects of groups with different steric requirements. For the purpose of ^{13}C ENDOR investigations we have synthesized several ^{13}C labeled compounds. ^{13}C hyperfine coupling constants are known to be very sensitive to structural changes within the carbon skeleton.[4] Finally measurements in liquid-crystalline solutions have been performed, yielding information about the anisotropic hyperfine interactions, especially of the ^{13}C nucleus. For comparison with the galvinoxyls similarly structured phenoxyls have been investigated. In this context we want to demonstrate that steric interactions may cause a drastic change of the magnetic behavior of the galvinoxyl system; strictly speaking, the galvinoxyl may tend to behave like a phenoxyl-type radical.

Experimental Section

The mass spectra were recorded on a CH 5-DF Varian-MAT spectrometer. The ^1H NMR spectra were recorded on a Varian XL 100. The ^{13}C NMR spectra were taken on a Bruker WH-270 with a 10-mm diameter sample tube and $CDCl_3$ or $CDCl_3/Me_2SO$-d_6 solvent.

The spectrometer used for ESR, ENDOR, and TRIPLE basically consists of a Bruker ER 220 D ESR spectrometer equipped with a Bruker cavity (ER 200 ENB) and home-built NMR facilities described elsewhere.[5] ENDOR spectra were accumulated by using a Nicolet Signal Averager 1170 employing 1K data points; typically 32 sweeps were taken, 30 s per scan. The temperature was varied with a Bruker B-VT 1000 temperature control unit, constant to ±1 K and checked by means of a thermocouple.

Preparation of Compounds. Previously we have shown that a variety of the precursors of galvinoxyl radicals, viz., the galvinols, can be obtained via an organometallic synthetic pathway.[6] According to this procedure carboxylic esters are treated with (2,6-di-*tert*-butyl-4-lithiophenoxy)trimethylsilane to give the respective carbinols. Subsequently the protecting trimethylsilyl groups are eliminated, yielding the galvinols. To obtain the ^{13}C labeled galvinols, the respective ^{13}C labeled carboxylic esters have been used, which were synthesized by a Grignard reaction from the appropriate halide and $^{13}CO_2$ followed by esterification. The galvinol **1c** was prepared by a cleavage reaction from tris(3,5-di-*tert*-butyl-4-hydroxyphenyl)methane-^{13}C.[7] The syntheses of the ^{13}C labeled galvinol **6c**[2] and the ketone **6e**[8] were described previously. The ^{13}C labeled ketone **5e** was obtained by the reaction between the ^{13}C labeled carboxylic acid, trifluoroacetic acid anhydride, and 2,6-di-*tert*-butylphenol.[9] The galvinol **2a** was recently synthesized by a different pathway.[10]

(3,5-Di-*tert*-butyl-4-hydroxyphenyl)(3,5-di-*tert*-butyl-4-oxocyclohexa-2,5-dienylidene)methane-^{13}C (1c). Bis(3,5-di-*tert*-butyl-4-

† Dedicated to Professor G. Manecke in honor of his 65th birthday.

(1) Hinrichs, K.; Kirste, B.; Kurreck, H.; Reusch, J. *Tetrahedron* **1977**, *33*, 151.
(2) Kirste, B.; Kurreck, H.; Lubitz, W.; Schubert, K. *J. Am. Chem. Soc.* **1978**, *100*, 2292.
(3) Kirste, B.; Kurreck, H.; Harrer, W.; Reusch, J. *J. Am. Chem. Soc.* **1979**, *101*, 1775.
(4) Fey, H.-J.; Lubitz, W.; Zimmermann, H.; Plato, M.; Möbius, K.; Biehl, R. *Z. Naturforsch. A* **1978**, *33A*, 514.
(5) Fey, H.-J.; Kurreck, H.; Lubitz, W. *Tetrahedron* **1979**, *35*, 905.
(6) Harrer, W.; Kurreck, H.; Reusch, J.; Gierke, W. *Tetrahedron* **1975**, *31*, 625.
(7) Kirste, B.; Kurreck, H.; Schubert, K. *Tetrahedron* **1980**, *36*, 1985.
(8) Lubitz, W.; Broser, W.; Kirste, B.; Kurreck, H.; Schubert, K. *Z. Naturforsch. A* **1978**, *33A*, 1072.
(9) Kreilick, R. W. *J. Am. Chem. Soc.* **1966**, *88*, 5284 and references cited therein.
(10) Colegate, S. M.; Hewgill, F. R. *Aust. J. Chem.* **1980**, *33*, 351.

0002-7863/81/1503-6280$01.25/0